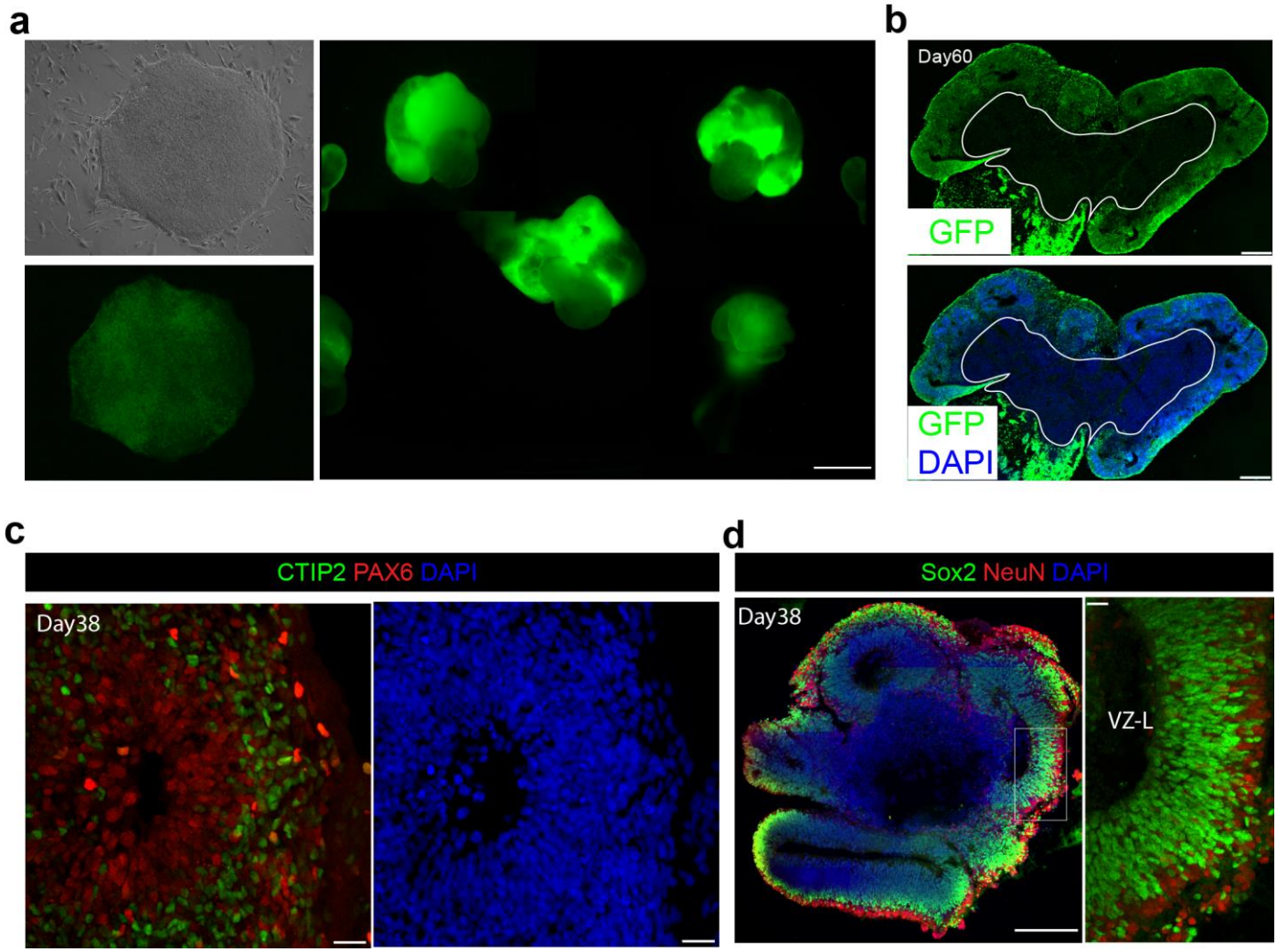

Supplementary Figure 1

Generation and characterization of GFP+ cerebral organoids.

(a) Microscopic image shows a single colony of H9-GFP+ hESCs (Left), and a representative example of 46-days old GFP+ brain organoids used for the transplantation experiments. **(b)** Immunofluorescence staining for GFP of GFP-expressing cerebral organoids at day 60. Note, unlike the perimeter areas, the center of the organoid-- lacks GFP expression. Solid line indicates the border of the low-GFP expressing region. **(c)** Cerebral organoids immunostained for PAX6 and CTIP2 at 38 days. **(d)** 38-days old cerebral organoids immunostained for SOX2 and NeuN. Right panel is magnification of the boxed area in the left panel. Scale bar is 1 mm in a, 200 μm in b, 20 μm in c, d (right), and 200 μm in d (left).

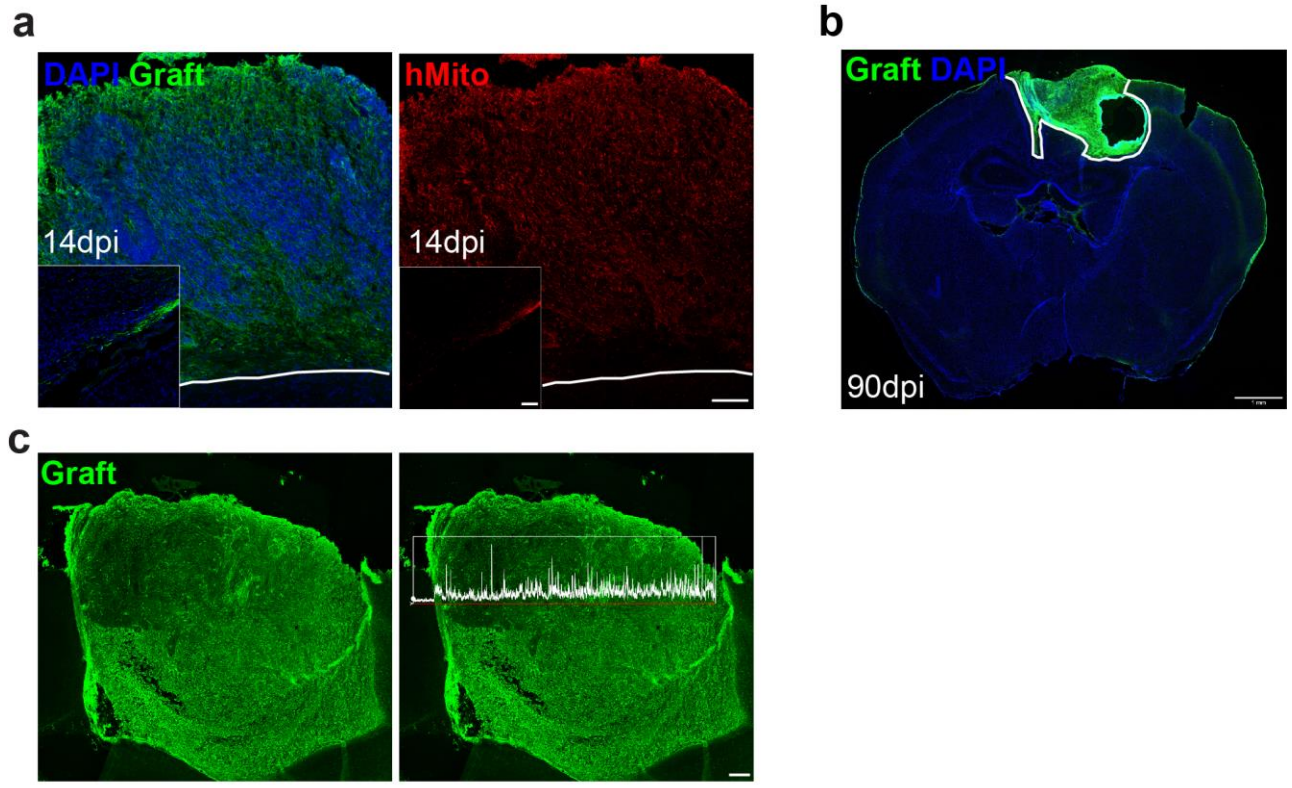

Supplementary Figure 2

In vivo long-term survival of grafted brain organoids.

(a) Immunofluorescence staining for GFP and human mitochondria (hMito), which specifically labels human cells, of the grafted brain organoid at 14 dpi. Insets show staining form the same section of neurites projection into the host brain. **(b)** Lower power slide scanner image of a coronal brain section stained with anti-GFP antibody showing robust integration of GFP^{+} human brain organoids at 90 dpi. Unlike organoids grown in culture before grafting (**Supplementary Fig. 1b)**, there are no detectable signs of regions that lack GFP expression in the center of the organoid 3 months post-implantation. **(c)** Left, confocal stitched tile scan of 90dpi-organoid graft stained with GFP. Right, Histogram of GFP intensity at various positions of the graft across the red line. Nuclei were counterstained with DAPI. Scale bar is, 100 μm in a, 1 mm in b, 200 μm in c.

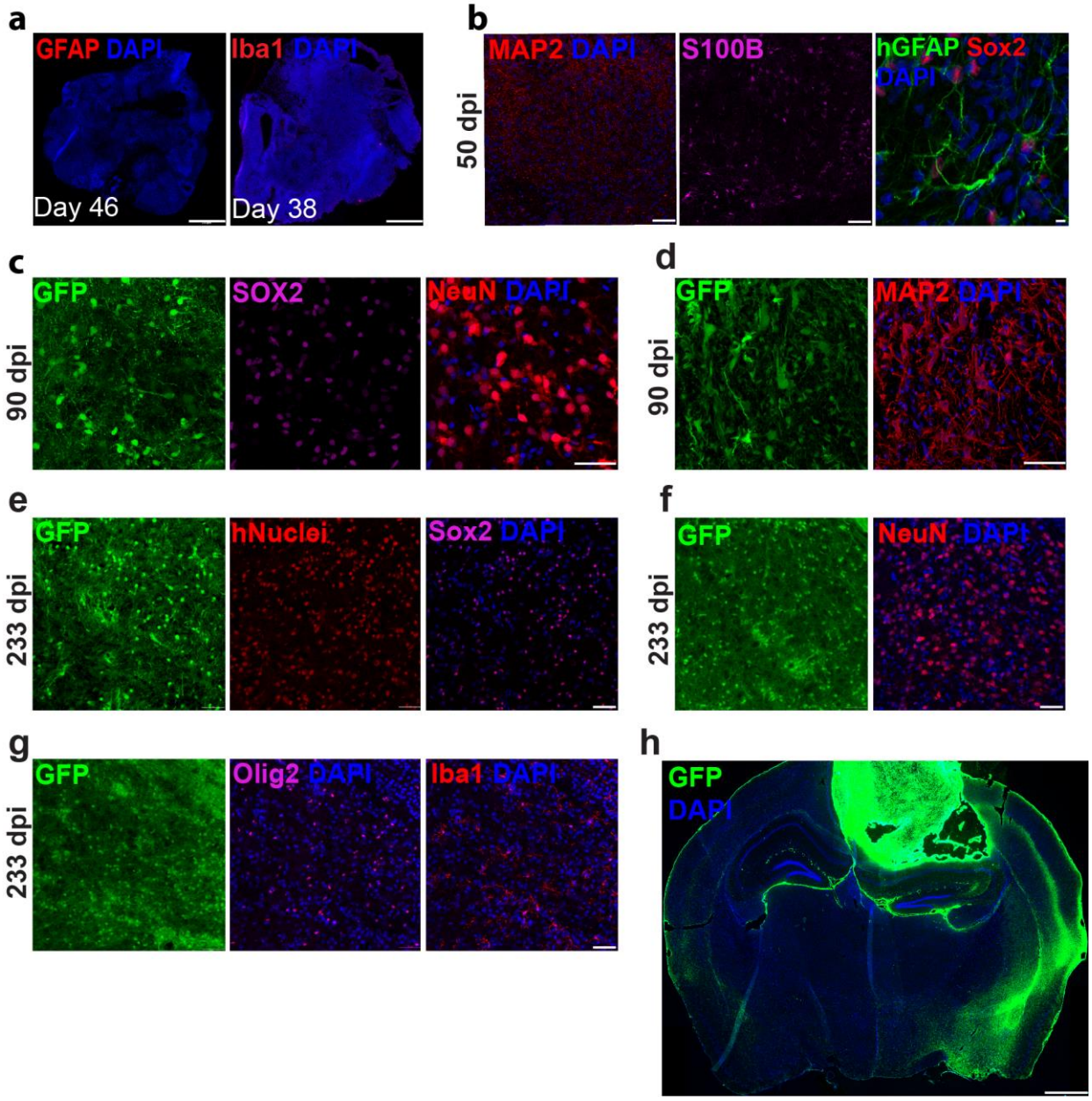

Supplementary Figure 3

In vivo neuronal differentiation of grafted brain organoids.

(a) Immunofluorescence staining for the mature astrocyte marker GFAP (left) and microglial marker Iba1 (right) on a whole organoid cross section at 46 days in culture. **(b)** Immunofluorescence staining of the mature neuronal dendrite marker MAP2 (left panel), astrocyte marker S100B (middle panel), and triple staining of GFP, hGFAP and SOX2 (right panel) inside the organoid graft at 50 dpi. Note the cellular colocalization between hGFAP and SOX2; co-association of SOX2 and hGFAP suggests that SOX2+ cells are glia and not NPCs.

(c) Immunofluorescence staining of GFP, Sox2, and NeuN within the grafted brain organoid at 90 dpi.**(d)** Immunofluorescence staining of GFP and MAP2 within the grafted brain organoid at 90 dpi. **(e)** Immunofluorescence staining of GFP, hNuclei, and SOX2 within the grafted brain organoid at 233 dpi. **(f)** Immunofluorescence staining of GFP and NeuN, within the grafted organoid at 233 dpi. **(g)** Immunofluorescence staining of GFP, Olig2, and Iba1 within the grafted brain organoid at 233 dpi. **(h)** Example image of coronal section obtained from grafted mouse brain at 90 dpi. Nuclei were counterstained with DAPI. Scale bar is, 500 μm in a, 50 μm in b-g, 1 mm in h.

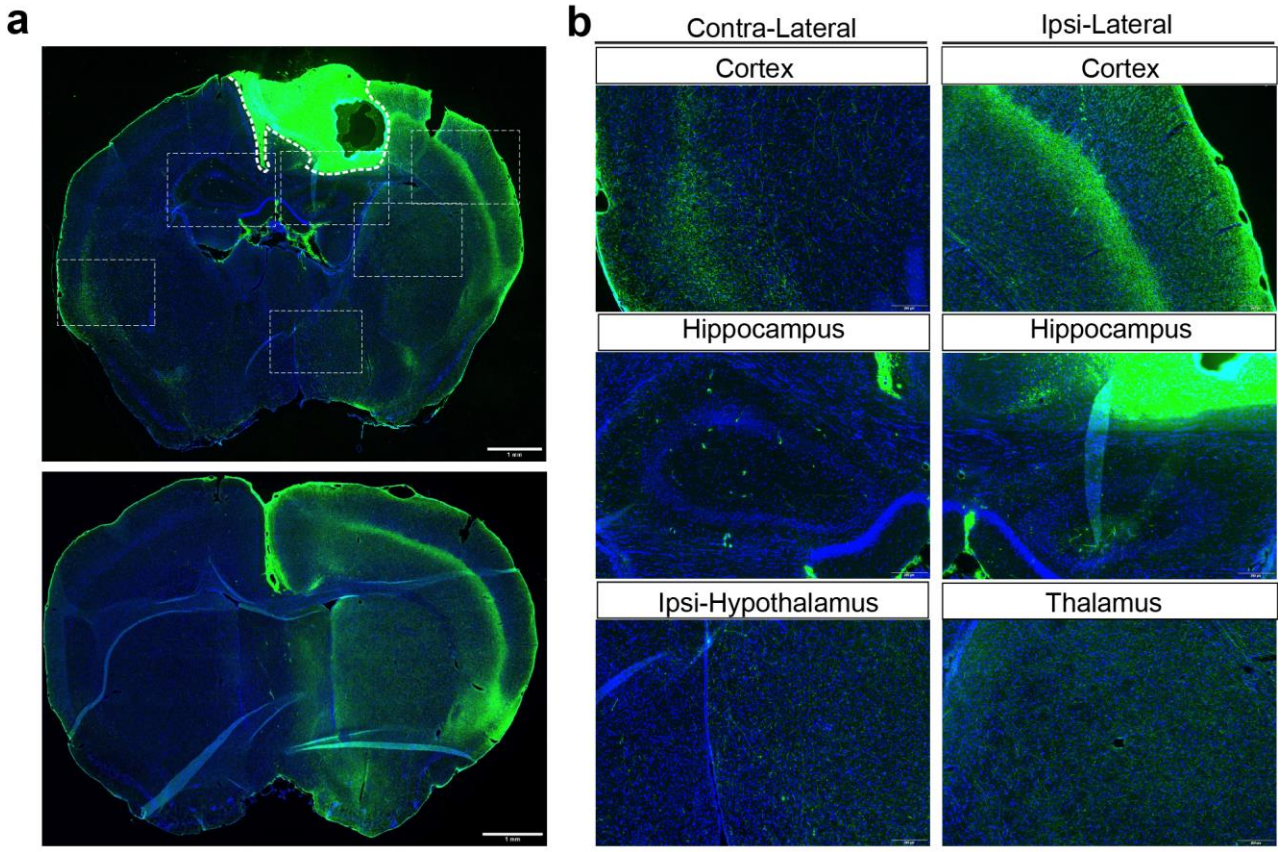

Supplementary Figure 4

Brain organoids send long-distance axonal projections with synaptic connectivity after implantation in mouse brain.

(a) Slide scanner images of coronal brain sections stained for GFP and obtained from 90-dpi grafted mouse brain show robust integration of GFP^+ organoids and very large numbers of axons extending into the grafting region and into more rostral section of the host brain. Dashed boxes indicate the sampled region from which higher magnification views in (**b**) were obtained. Note that images were over-saturated for the signal in the graft region to show the GFP signal in the axons trajectories. Note that the high background on the edge of the section is a nonspecific signal. Scale bars:1 mm in a and 200 μm in b.

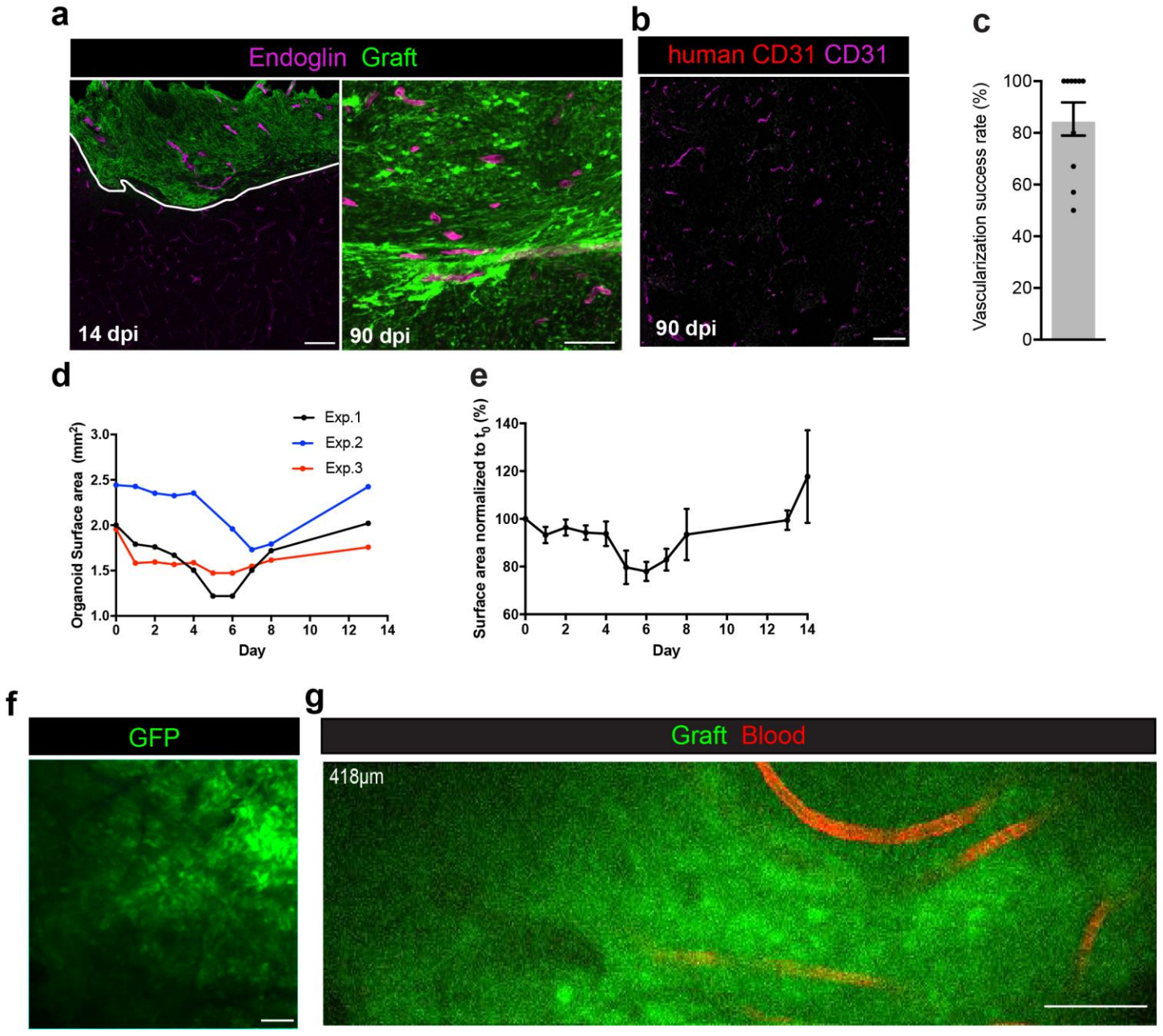

Supplementary Figure 5

Vascularization and two-photon imaging of the organoid graft.

(a) Double immunofluorescence staining of GFP and the endothelial marker Endoglin in the indicated post-implantation stage showing the intensive growth of blood vessels inside the organoid graft. **(b)** Double immunofluorescence staining for human-specific CD31 and CD31 (recognizing both mouse and human) of organoid graft harvested at 90 dpi. Note that the organoid graft is negative for human CD31, suggesting a host origin of the infiltrated blood vessels at the examined time point. **(c)** Quantification of vascularization success rate in the grafted organoids. Average value is 85.4%±6.4; data represent mean±s.e.m (n=10 independent experiments, total of 55 animals). **(d)** Surface area change of single grafted organoids during the first 2 weeks of implantation. **(e)** The average change of total organoid surface area during the first 2 weeks of implantation normalized to day 0 (100%). Data represent mean ± s.e.m from at least 3 grafted animals; day 0-5 (n=9), day 6 (n=8), day 7 and 8 (n=6), day 13 (n=4), day 14 (n=3). **(f)** Deep *in vivo* two-photon imaging of GFP signal of the implanted organoids in a head-fixed awake mouse through the cranial window, demonstrating the feasibility of the imaging system. Image shows maximum projection of 300 µm from 200-500 µm inside the grafted organoid from a 30 dpi mouse. **(g)** Two-photon imaging of blood vessels inside the grafted organoid. Dextran was infused in engrafted animal at 120 dpi. Single z-plane acquired at 418 µm depth below the organoid surface, showing blood flow inside the vascular network (see Supplementary video 4). Scale bar is 50 µm in a,b and 100 µm in h,g.

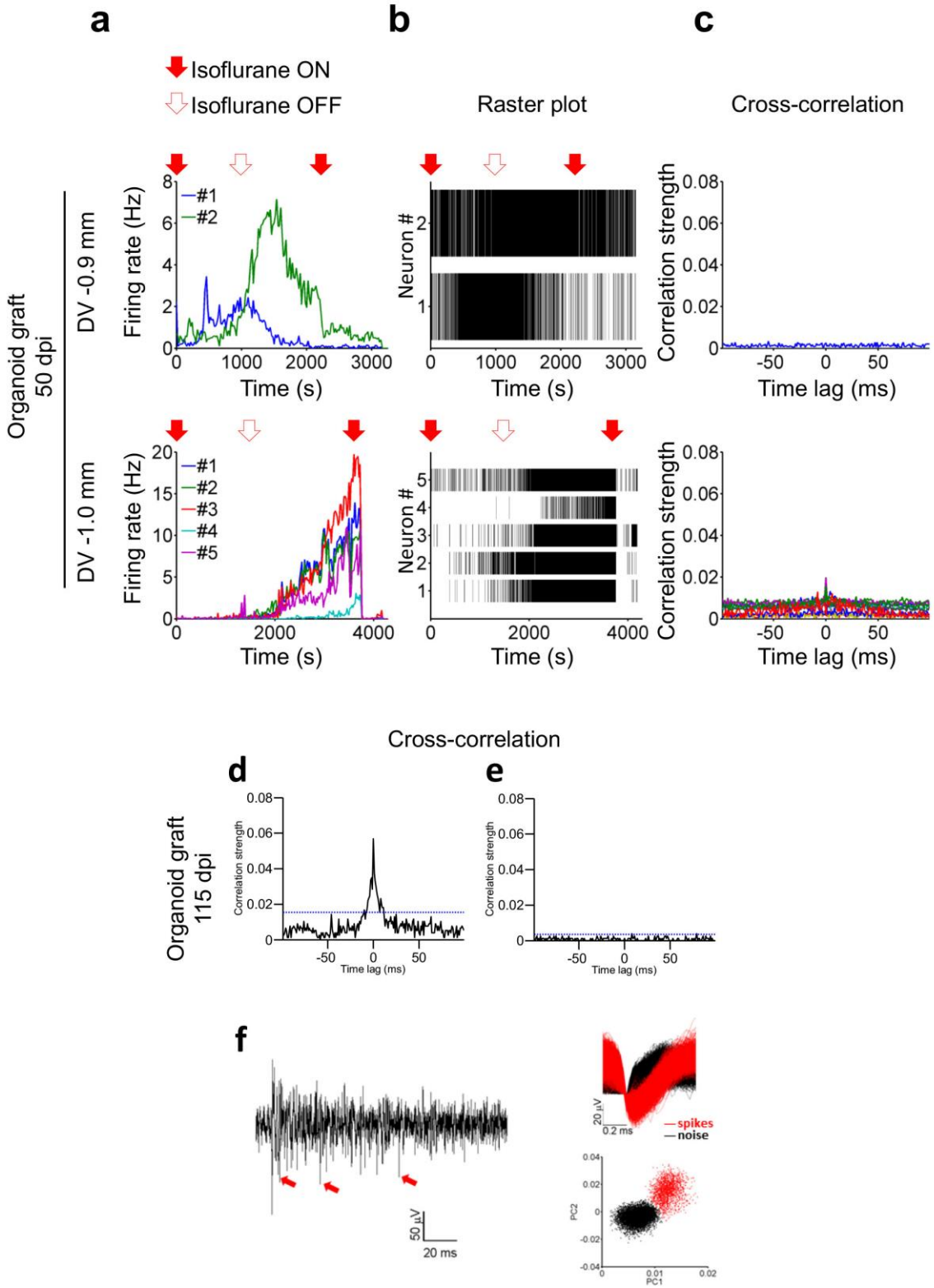

Nature Biotechnology: doi:10.1038/nbt.4127

Supplementary Figure 6

Electrophysiological recording of neuronal activity in the grafted brain organoids.

(a) Firing rate changes of single neurons obtained from 50-dpi organoid at two different levels of depth (top: -0.9 mm; bottom: -1.0 mm) from the graft surface. Each line (color-coded) indicates the firing rate of an individual neuron. Arrows on the top denote the time isoflurane was turned ON (filled arrows) and OFF (empty arrows). **(b)** Spike raster plots from the neurons in (a) at two different depths (top: -0.9 mm; bottom: -1.0 mm). Each vertical bar indicates a single spike. **(c)** Cross-correlation of neuron pairs in (a) at depths of -0.9 mm (top) and -1.0 mm (bottom). **(d,e)** Example of cross correlation analysis performed on one neuron pair from a 115 dpi organoid graft (Fig. 6f). Analysis was performed by testing the significance of the central peak observed in cross-correlation (d). The threshold for the test was calculated based on mean + 3*SD of the baseline, which was defined as the time window from -100 ms to -20 ms in cross-correlation (d, dashed blue line). Obviously, although the magnitude is relatively small, the central peak significantly exceeds the threshold, which is evident of correlation between neurons. Note that when shuffling the neuronal activity with a random duration, the shuffled cross-correlation between the same neurons in (d) became completely flat with no peak (e), indicating that the correlation is indeed from the correlated activity, rather than noise. (**f**) Spikes with magnitude exceeding the threshold were tagged and recorded as waveforms (red arrows). Then we applied PCA analysis to these waveforms to discriminate the neuronal spikes from noise. On PC plane, waveforms showing distinct shapes are classified into separate clusters.

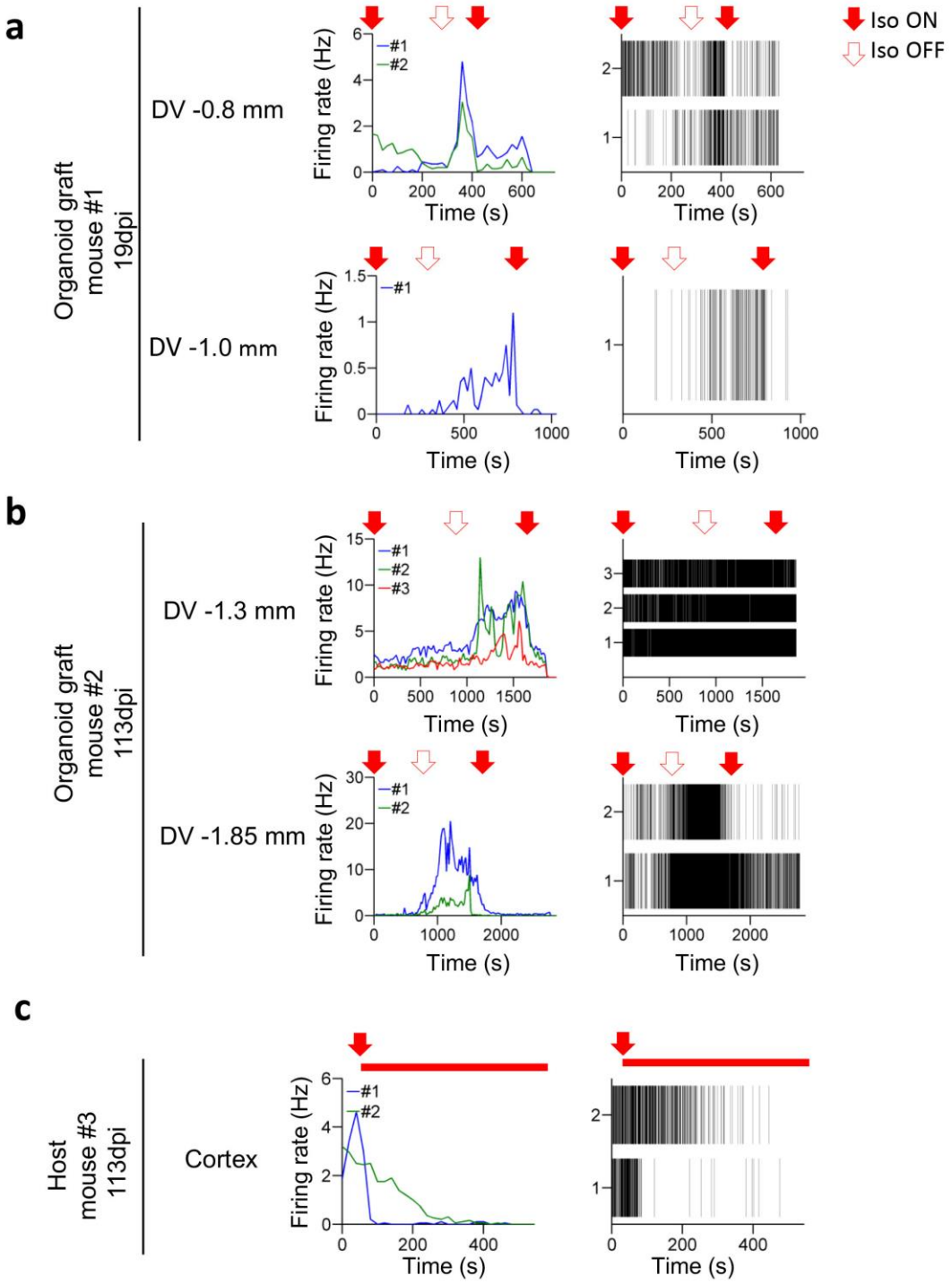
a
Organoid graft
mouse #1
19dpi
DV -0.8 mm
DV -1.0 mm
Firing rate (Hz)
Time (s)
#1
#2
Iso ON
Iso OFF
b
Organoid graft
mouse #2
113dpi
DV -1.3 mm
DV -1.85 mm
#3
c
Host
mouse #3
113dpi
Cortex

Supplementary Figure 7

Electrophysiological recording of neuronal activity in the grafted brain organoids.

Examples of *in vivo* recording from the organoid graft and the host brain. **(a-b**) Left panels, firing rate changes of single neurons obtained from the indicated time points and the dorsal-ventral (DV) depth from the graft surface. Each line (color-coded) indicates the firing rate of an individual neuron. Arrows on the top denote the time isoflurane was turned ON (filled arrows) and OFF (empty arrows). Right panels, spike raster plots from the neurons in the left panel. Each vertical bar indicates a single spike. **(c)** Firing rate changes of single neurons obtained from the host cortical region.

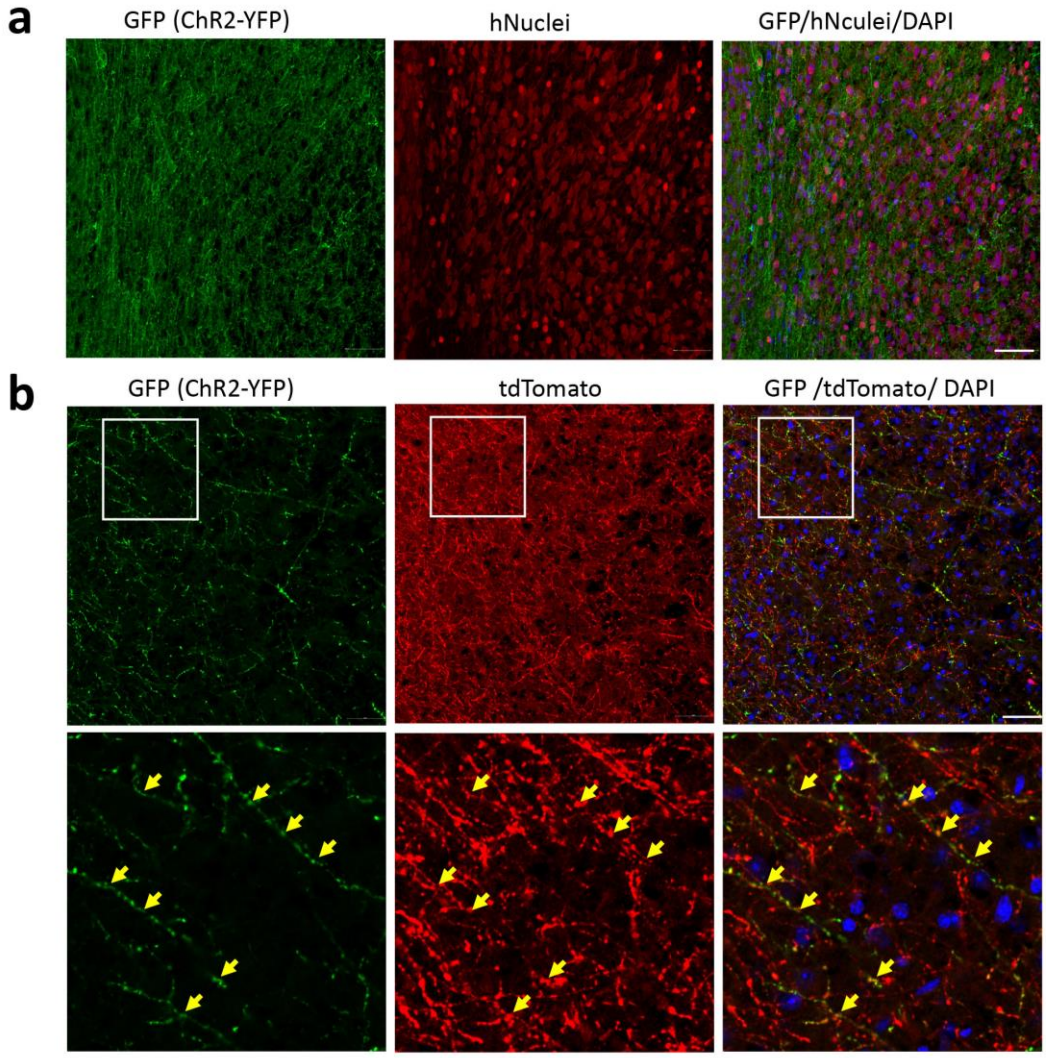

Supplementary Figure 8

Transduction of ChR2 into the grafted organoid for optogenetic stimulation.

Organoid graft was injected with AAV-hSyn-ChR2-YFP and analyzed at 155 dpi. **(a)** Immunostaining for GFP (labeling hSyn::ChR2-YFP) and hNuclei inside the organoid graft. **(b)** Immunostaining for tdTomato (labeling organoid graft) and GFP (labeling hSyn::ChR2-YFP) in the cortex of the host brain at 155 dpi. Bottom panels are magnification of the boxed area in the top panel. Note the fragmented tdTomato expression along the axons perhaps due to long term expression. Nuclei were counterstained with DAPI. Scale bar is 50 μm.

Nature Biotechnology: doi:10.1038/nbt.4127

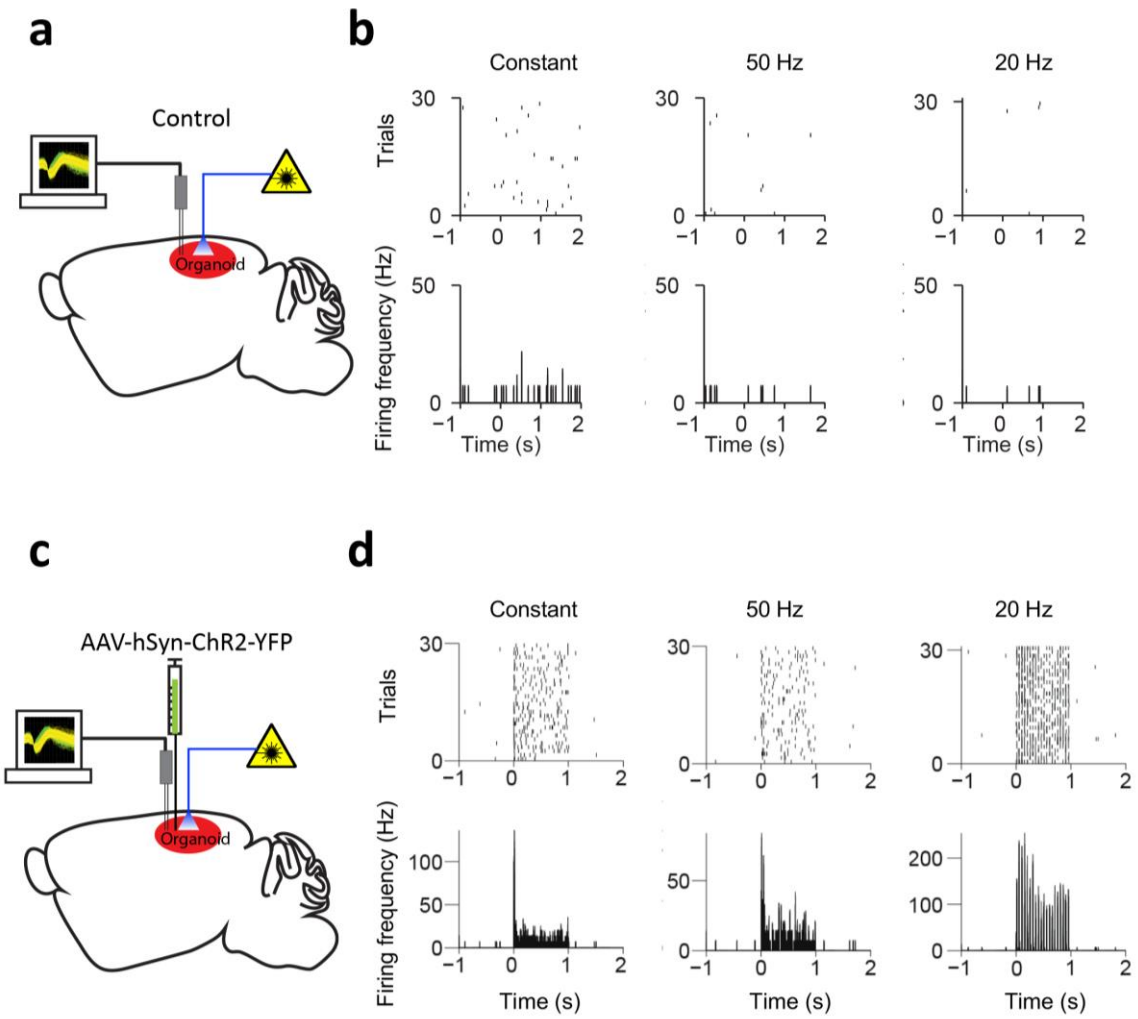

Supplementary Figure 9

Optogenetic stimulation evokes neuronal responses in the organoid-graft expressing ChR2.

(a) Diagram of optogenetic stimulation and electrophysiological recording in un-injected control organoid-graft. **(b)** Light-evoked responses from the same single neuron to 1s constant (left panel), 50 Hz (middle panel), or 20 Hz (right panel) light stimulation in control graft. Top panels: raster plot of neuronal responses in 30 trials. Each tick indicates a single spike. Bottom panels: PETH of the average firing rate across 30 trials. **(c,d)** Organoid graft was injected with AAV-hSyn-ChR2-YFP and analyzed at 155dpi. **(c)** Diagram of optogenetic stimulation and electrophysiological recording in organoid graft. **(d)** Light-evoked responses from the same single neuron to 1s constant (left panel), 50 Hz (middle panel), or 20 Hz (right panel) light stimulation. The stimulation onset is at 0. Top panels: raster plot of neuronal responses in 30 trials. Each tick indicates a single spike. Bottom panels: PETH of the average firing rate across 30 trials. The response latency to the laser onset was less than 5 milliseconds and no detectable response was observed before or after the period of light illumination. n= 2 animals. All recordings were performed while animals were under isoflurane anesthesia.

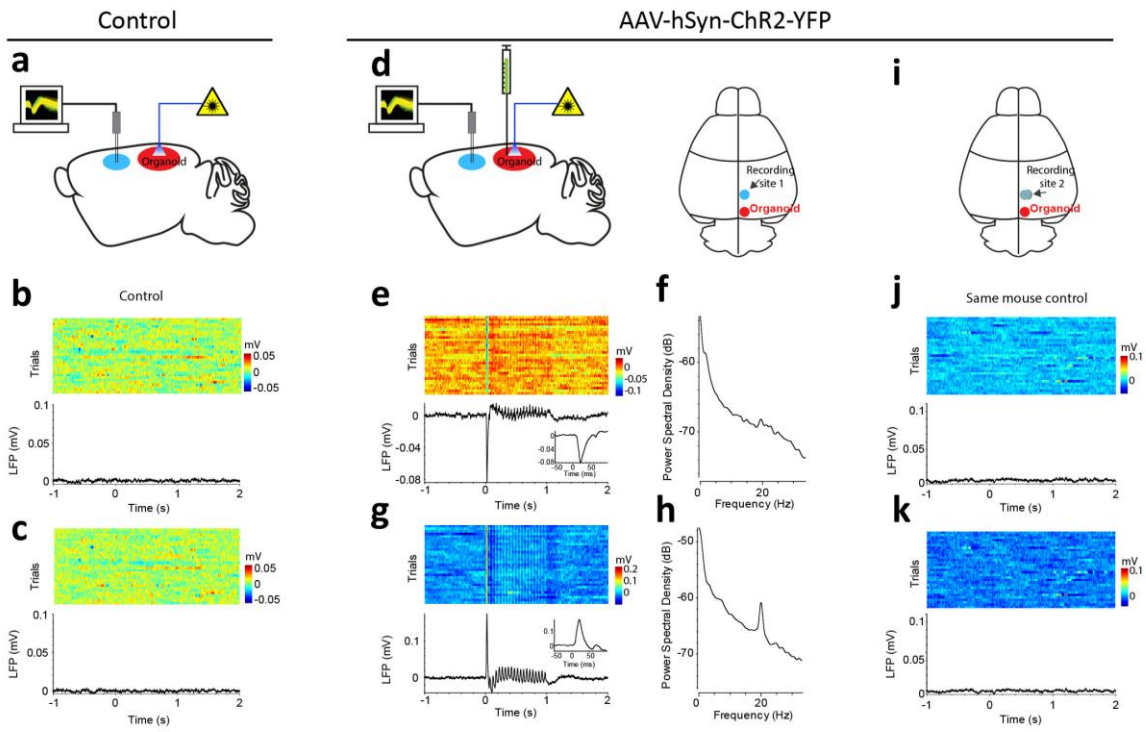

Supplementary Figure 10

Optogenetic stimulation reveals intragraft neuronal activity and functional output connectivity from the organoid graft to host brain.

(a) Diagram of optogenetic stimulation in tdTomato-expressing uninfected-control organoid and electrophysiological recording in the host brain. **(b)** Local field potential (LFP) recorded from a single electrode in the control host brain after optogenetic stimulation of organoid with 20 Hz light stimulation. The voltage is color coded for 30 trials (top). Averaged LFP across trials (bottom). **(c)** LFP changes recorded from a different electrode from the same brain region in (b). **(d-h)** Organoid graft was injected with AAV-hSyn-ChR2-YFP and analyzed at 155dpi. **(d)** Diagram of optogenetic stimulation in tdTomato-expressing, AAV-hSyn-ChR2-YFP-infected, organoid and electrophysiological recording in the host brain (fiber location: DV -1.7mm; array location: AP -2.54 mm, ML -1.5 mm, DV -2.2 mm). **(e)** Local field potential recorded from a single electrode in the host brain region. Optogenetic stimulation of organoid with 20 Hz drives LFP changes in the host brain region. The voltage is color coded for 30 trials (top). Averaged LFP across trials (bottom). Inset: Averaged LFP with a finer time scale. **(f)** Power spectral density of the averaged LFP in (e). **(g)** LFP changes recorded from a different electrode from the same brain region in (e). Inset: Averaged LFP with a finer time scale. **(h)** Power spectral density of the averaged LFP in (g). **(i-k)** LFP changes recorded from the same animal and brain region as in (d) but from different, more dorsal array location (AP -2.54 mm, ML -1.5 mm, DV -0.8mm). n=2 animals. All recordings were performed while animals were under isoflurane anesthesia.

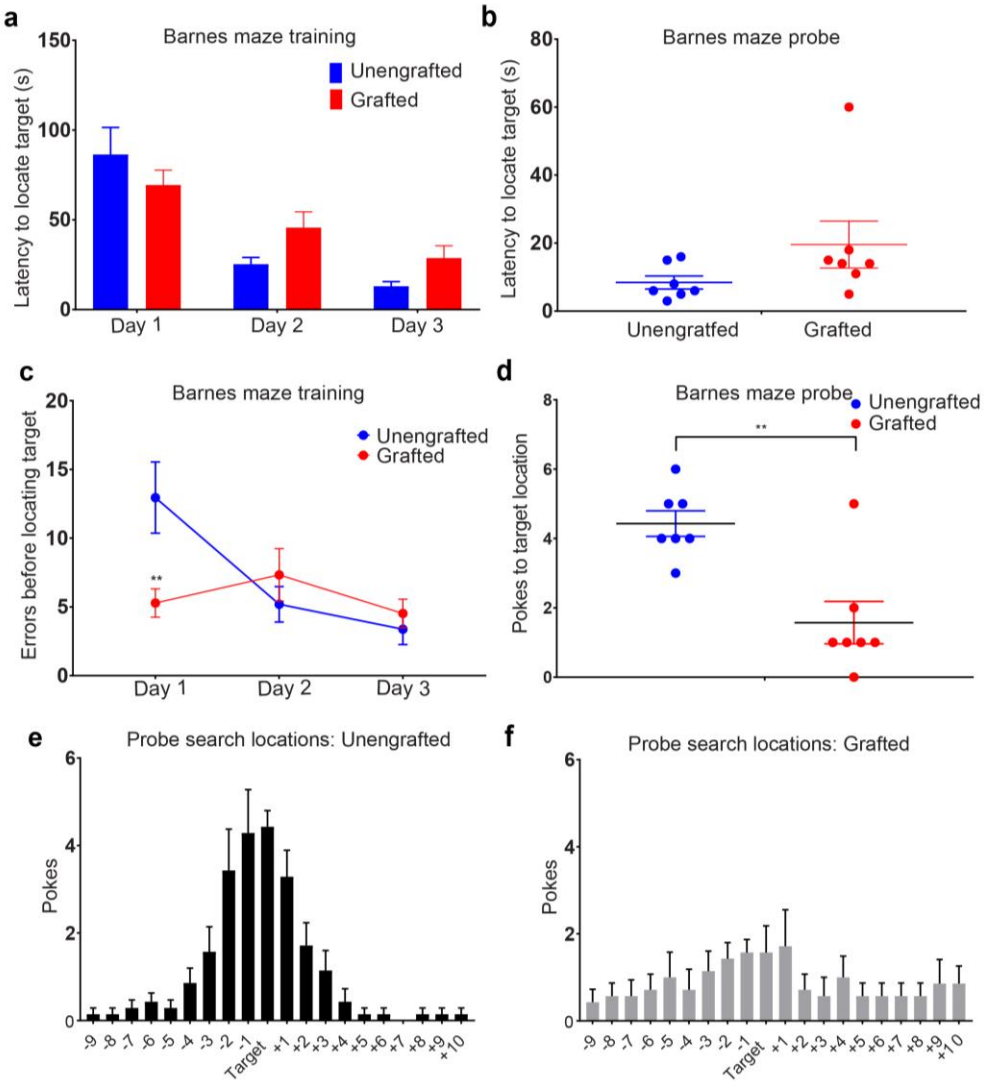

Supplementary Figure 11

Behavioral examination of spatial learning abilities in organoid-grafted mice

(a) Latency to locate target during Barnes maze training of 3 trials per day for 3 days. Values for individual mice were averaged within each day for analysis. Training performance was analyzed by two-way ANOVA with group as a between subject factor and day as a within-subject factor. There was a significant effect of day ($F(2,24) = 24.3$, $p < 0.0001$), but no effect of group ($F(1,12) = 0.8116$, $p = 0.3854$) or group X day interaction ($F(2,24) = 2.878$, $p = 0.0758$). **(b)** Latency to locate target during Barnes maze probe trial on day 4, 24 hr after final training day. Probe trial performance was analyzed by the Mann-Whitney test. Unengrafted vs. grafted $p = 0.1474$. **(c)** Errors prior to locating target during Barnes maze training of 3 trials per day for 3 days. Values for individual mice were averaged within each day for analysis. There was a significant effect of day ($F(2,24) = 7.244$, $p = 0.0035$) and a group X day interaction ($F(2,24) = 7.878$, $p = 0.0023$; **post-hoc Sidak's multiple comparison test $p = 0.0052$ for training Day 1, $p = 0.7258$ for Day 2, $p = 0.9438$ for Day 3). No main effect was observed for group ($F(1,12) = 0.8008$, $p = 0.3884$). **(d)** Pokes to target location during Barnes maze probe trial on day 4, 24 hr after final training day. **Unengrafted vs. grafted $p = 0.0076$ **(e)** Location of errors during probe trial for Nod-Scid mice. **(f)** Location of errors during probe trial for organoid implanted mice. Values in a-f represent mean ± s.e.m. for each group, n=7 mice per group.